# Pathological axonal enlargement in connection with amyloidosis, lysosome destabilization and hemorrhage is a major defect in the Alzheimer's disease

Hualin Fu[1, 2, 3*], Jilong Li[1], Chunlei Zhang[1, 3], Guo Gao[1, 3], Qiqi Ge[2, 4], Xinping Guan[4, 5], Daxiang Cui[1, 3]

**Affiliations:**

[1]Institute of Nano Biomedicine and Engineering, School of Sensing Science and Engineering, School of Electronic Information and Electrical Engineering, Shanghai Jiao Tong University, 800 Dongchuan Road, Shanghai, 200240, China

[2]Institute of Marine Equipment, Shanghai Jiao Tong University, 211 Wenjin Road, Shanghai, 200240, China

[3]National Center for Translational Medicine, Shanghai Jiao Tong University, 800 Dongchuan Road, Shanghai, 200240, China

[4]Department of Automation, Shanghai Jiao Tong University, Shanghai 200240, China

[5]The Key Laboratory of System Control and Information Processing, Ministry of Education, Shanghai 200240, China

*Correspondence to: hfu@sjtu.edu.cn or 1010720220@qq.com (Hualin Fu)

**Abstract:** Alzheimer's disease (AD) is a multi-amyloidosis disease with Aβ deposits in the cerebral blood vessels, microaneurysms and senile plaques. How Aβ amyloidosis affects axon pathology is not well-examined. We studied the Aβ-related axonal phenotypes in the AD brains with histochemistry, immunohistochemistry and fluorescence imaging. We found that widespread axonal amyloidosis existed in the AD brain tissues with a distinct axonal enlargement phenotype. Aβ-positive axon diameters

in AD brain tissues were 1.72 times as large as control brain axons by average and they showed a significant loss of axonal structural protein MAP2. Axonal amyloidosis was also associated with Tau phosphorylation and lysosome destabilization. In addition, axonal amyloidosis bore the markers of hemorrhagic insults such as ApoE, HBA, HbA1C, and Hemin. Under extreme conditions, axon breakage was observed, which likely results in Wallerian degeneration in some axons. We believe that axonal amyloidosis and enlargement associated with chronic microhemorrhage and lysosome destabilization is a major neurological defect in the Alzheimer's disease.

**Keywords**: axonal enlargement; lysosome destabilization; Aβ; Tau; hemoglobin; Wallerian degeneration; Alzheimer's disease

## Introduction：

The pathological hallmarks of Alzheimer's disease include senile plaques, neurofibrillary tangles and neuritc dystrophy[1, 2]. Neuritc dystrophy refers to the dystrophy of axons and dendrites. In our previous investigation, we identified cerebral microaneurysm rupture and hemolytic Aβ leakage as a pathological mechanism for senile plaque formation[3]. Yet, how chronic hemolytic leakage impacts on other pathological phenotypes such as axonal dystrophy in the Alzheimer's disease is not well-studied. Previous studies implicated that both Aβ and Tau phosphorylation are involved in the axonal defects in Alzheimer's disease[4-6]. However, the exact linkage between Aβ, Tau and their contribution to axonal dystrophy is not clear.

In the current study, we analyzed the pathological phenotypes in axons in the AD brain tissues by immunohistochemistry, histochemistry and fluorescent imaging methods. The results showed that the major axonal phenotype in Alzheimer's disease (AD) is the widespread axonal amyloidosis and enlargement with additional spheroid formation. The axonal defect in AD is associated with the enrichment of Aβ, phos-Tau, destabilized

lysosomes and hemorrhage-related proteins in axons.

## MATERIAL AND METHODS

**Tissue sections**. AD patient frontal lobe brain paraffin tissue sections were purchased from GeneTex (Irvine, CA, USA). Additionally, AD patient and non-AD control frontal lobe brain paraffin tissue sections were provided by National Human Brain Bank for Development and Function, Chinese Academy of Medical Sciences and Peking Union Medical College, Beijing, China. This study was supported by the Institute of Basic Medical Sciences, Chinese Academy of Medical Sciences, Neuroscience Center, and the China Human Brain Banking Consortium. All procedures involving human subjects are done in accord with the ethical standards of the Committee on Human Experimentation in Shanghai Jiao Tong University and in accord with the Helsinki Declaration of 1975.

**List of antibodies for immunohistochemistry**. The following primary antibodies and dilutions have been used in this study: Aβ (Abcam ab201061, 1 : 200, Cambridge, UK), Aβ/AβPP (CST #2450, 1 : 200, Danvers, MA, USA), phos-TAU (Abcam ab151559, 1:200), MAP2 (Proteintech 17490-1-AP, 1:200, Rosemont, IL, USA), ApoE (Abcam ab183597, 1:200), Sortilin1 (Abcam ab263864, 1:200), HBA (Abcam ab92492, 1:200), Cathepsin D (Abcam ab75852, 1:200), Lamp2 (Proteintech, 66301-1-Ig, 1:100), HbA1c (OkayBio K5a2, 1 : 100, Nanjing, Jiangsu, China), Hemin (Absolute Antibody, 1D3, 1 : 100, Redcar, UK), AGE (Advanced Glycation End Products) (Abcam, ab23722, 1:200). The following secondary antibodies and dilutions have been used in this study: donkey anti-mouse Alexa-594 secondary antibody (Jackson ImmunoResearch 715-585-150, 1:400, West Grove, PA, USA), donkey anti-rabbit Alexa-488 secondary antibody (Jackson ImmunoResearch 711-545-152, 1:400), donkey anti-rabbit Alexa-594 secondary antibody (Jackson ImmunoResearch 711-585-152, 1:400), and donkey anti-mouse Alexa-488 secondary antibody (Jackson ImmunoResearch 715-545-150, 1:400).

**Immunohistochemistry** was performed as described[7]. Briefly, paraffin sections were deparaffinized by Xylene, 100% EtOH, 95% EtOH, 75% EtOH, 50% EtOH, and PBS washes. Sections were then treated with 10 mmol/L pH 6.0 sodium citrate or 10 mmol/L pH 9.0 Tris-EDTA antigen retrieval solutions in a microwave at high power for 5 min to reach the boiling point and then at low power for another 15 min. The sections were allowed to naturally cool down to room temperature. Then, the slides were blocked with TBST 3% BSA solution for 1 hour at room temperature. After blocking, the samples were incubated with primary antibodies at room temperature for 2 hrs followed by 5 washes of TBST. After that, the samples were incubated with fluorescent secondary antibodies overnight at 4 degree. The treated samples were washed again with TBST 5 times the second day and mounted with PBS+50% glycerol supplemented with Hoechst nuclear dye (Sigma, B2261, 1 μg/ml) and ready for imaging. IHC experiments without primary antibodies were used as negative controls. All experiments have been repeated in order to verify the reproducibility of the results.

**Rhodanine staining**: The Rhodanine staining kit (BA4346) was purchased from Baso Diagnostics Inc. (Zhuhai, China). Briefly, paraffin sections were first deparaffinized as described above. After a quick wash in 95% ethanol, the slides were stained in the Rhodanine staining solution (0.01% p-Dimethylaminobenzalrhodanine) in a 37-degree incubator for 30 minutes. After staining, the slides were treated with a 95% ethanol quick wash and 5 times wash in water, then mounted with PBS+50% glycerol solution for imaging analysis.

**Alizarin Red staining**: The Alizarin Red staining kit C0138 was purchased from Beyotime Biotechnology (Shanghai, China). Briefly, paraffin sections were deparaffinized as described above. Then, the slides were stained in the Alizarin Red staining solution (2%, pH4.2) for 5 minutes at room temperature. After staining, the sections were washed 5 times with water, then mounted with PBS+50% glycerol solution for imaging.

**Imaging and morphometry analysis**. The fluorescent images were captured with a CQ1 confocal fluorescent microscope (Yokogawa, Ishikawa, Japan) and the color images of sections with histological stains were taken with an Olympus IX71 fluorescent microscope (Olympus Co., Toyoko, Japan). There is a difference in terms of exposure settings when imaging axonal staining versus senile plaque staining. To image axonal Aβ staining clearly, the exposure time should be increased significantly. Images were then analyzed with ImageJ software (NIH, USA). When comparing signal intensities with the same exposure settings, the mean area density was used as the parameter to define the marker densities. The perimeters of axons in transverse orientations were measured to simplify the axon diameter estimation by using the following formula: diameter = perimeter/3.14. The diameters of axons could also be measured directly with the ImageJ line tool utilizing the microscopy scale as a reference.

**Statistics**. All data first went through a Shapiro & Wilk normality test using SPSS Statistics 19 software. Two-tailed unpaired T-test was used to compare the means of data with a normal distribution with Excel 2007 software. For data that were not normally distributed, nonparametric Mann-Whitney test was performed to compare the means by using SPSS Statistics 19 software. For the correlation analysis, Pearson correlation was used for the data with a normal distribution while Spearman correlation was used for the data that were not normally distributed. The p Value threshold for statistical significance is set at 0.05. If $p<0.05$, then the difference was considered statistically significant. When $p<0.001$, it was labeled as $p<0.001$. If $p \geqq 0.001$, then the p Value was shown as it was.

**Funding**: This work was supported by the National Natural Science Foundation of China (81472235), the Shanghai Jiao Tong University Medical and Engineering Project (YG2021QN53, YG2017MS71), the International Cooperation Project of National Natural Science Foundation of China (82020108017), and the Innovation Group Project of National Natural Science Foundation of China (81921002).

**Author contributions:** HF conceived the study, designed and supervised the experiments and wrote the manuscript; HF, JL performed the experiments; HF, JL, CZ, GG, QG, XG and DC did the data analysis; all authors reviewed the manuscript.

**Competing interests:** Authors declare no competing interests.

**Data availability statement:** The data that supports the findings of this study are available from the corresponding author upon request.

**Supplementary Materials.** Supplementary Figures 1, 2

**Acknowledgements**: We want to thank the help from Dr. Ma Chao and Dr. Qiu Wenying for providing AD tissue sections from National Human Brain Bank for Development and Function, Chinese Academy of Medical Sciences and Peking Union Medical College, Beijing, China. Additionally, we want to thank Dr. Ming Yang from Shanghai Jiao Tong University, Dr. Xiangli Zhang from Shandong University, Dr. Peng Du and Dr. Lei Xia from Xinhua Hospital for valuable scientific discussions. Moreover, we want to thank Housheng Wang, Pingxin Liu, Xiaoyi Bao, and Jun Wang for excellent laboratory assistance.

## Results:

### Axon amyloidosis and enlargement in AD brain tissues

In our previous publications, Aβ staining was detected in senile plaques, CAA, neurons and red blood cells[3, 8]. After careful re-examining of the Aβ staining patterns in the AD brain sections with optimized staining condition and longer exposure settings, we found that there were clear axon-specific Aβ staining patterns that we previously did not recognize. Figure 1A showed that axon amyloidosis is widespread in AD brain tissues. Aβ immunostaining was distributed along the length of many axons. Aβ-

positive axons can be observed both around senile plaques or without senile plaques in the vicinity. Axonal amyloidosis could be detected in axons at both longitudinal and transverse orientation. Axons with Aβ staining were often shown as grouped clusters, corresponding to the known structural character in the human brain cortex as “axonal bundles”. Additionally, puff-like spheroid formation can be detected in a subset of the Aβ-positive axons. Spheroids are often formed at positions with enhanced Aβ staining. Aβ-positive axons have a general enlargement phenotype (Figure 1B), which is a basic character appearing more frequently than the spheroid formation. The diameters of Aβ-positive axons in the transverse orientation outside of senile plaque regions were measured since the strong plaque Aβ staining precludes the accurate identification of Aβ-positive axons within the senile plaques. The measured Aβ-positive axons had an average diameter of 1.94±0.59 μm (N=200) while MAP2-labeled axons from control front brain samples measured around 1.13±0.39 μm (N=34). In another word, Aβ-positive axon diameters were around 1.72±0.52 fold of control axons ($p<0.001$). In addition, among AD axon samples, the mean Aβ staining intensity was weakly positively related to the axon diameter ($r=0.338$, $p<0.001$, N=200, Spearman correlation), further emphasizing the positive influence of Aβ on the size enlargement of axons. The data suggested that the Aβ-amyloidosis associated axonal enlargement is a basic pathological phenotype in the Alzheimer’s disease.

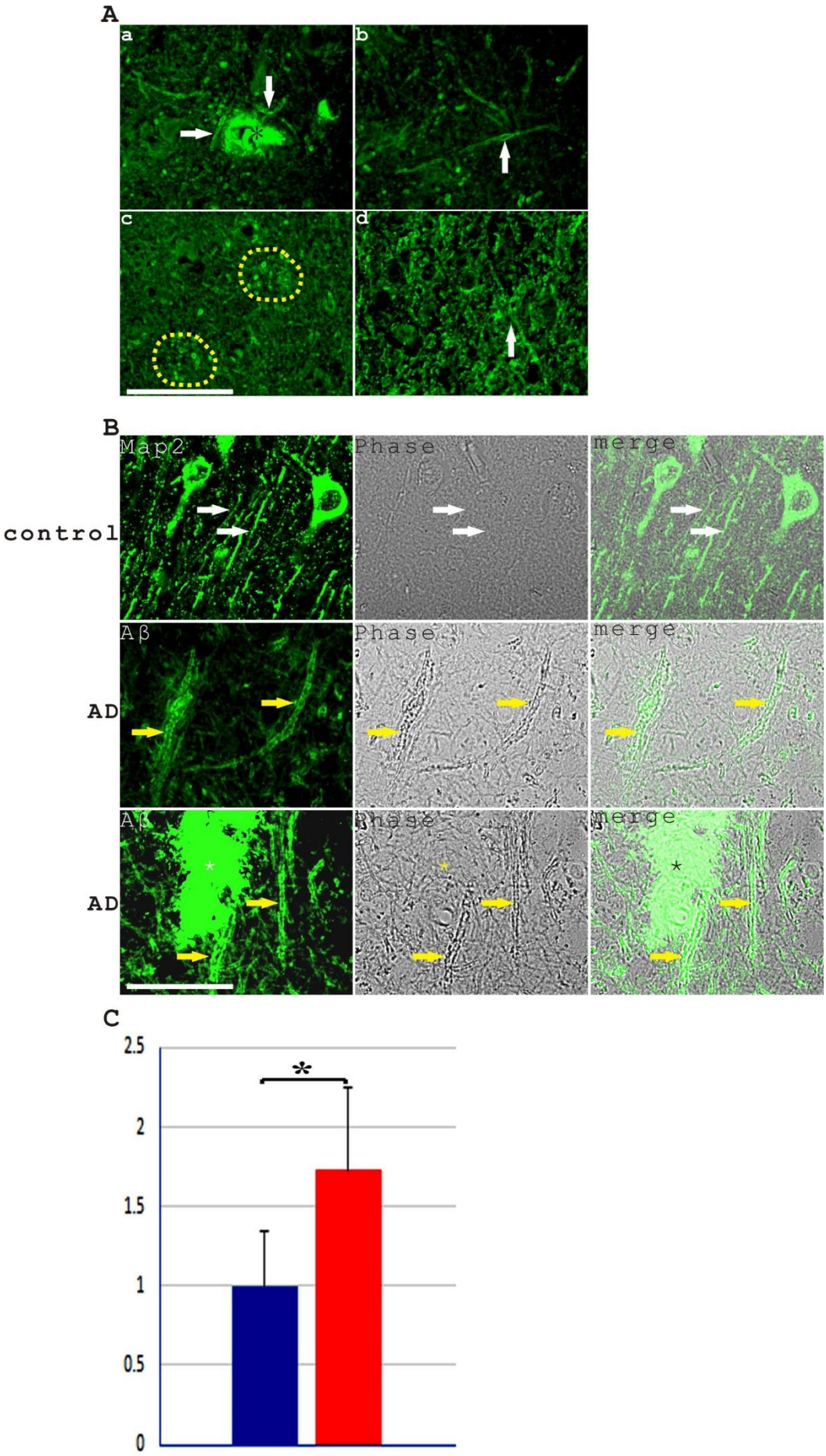
A
a
b
c
d
B
Map2
Phase
merge
control
Aβ
Phase
merge
AD
Aβ
Phase
merge
AD
C
2.5
2
1.5
1
0.5
0
*

**Figure 1: Axon amyloidosis and enlargement are important pathological phenotypes in the Alzheimer's disease. A.** Axon amyloidosis was detected in AD frontal brain tissues with Aβ antibody with green fluorescence. a, Aβ expression was detected both in a senile plaque (indicated with an asterisk) and in axons (indicated with arrows). b, An axon at the longitudinal orientation showed spheroid formation stained with Aβ antibody (indicated with an arrow). c, Two clusters of Aβ-positive axons (indicated by dashed lines) were shown, indicating Aβ staining of axon bundles. d, Abundant axon Aβ staining was detected in the white matter with one axon indicated by an arrow. Scale bar, 50 μm. **B**. A general enlargement of axons in AD brain tissues was observed when comparing control axons (indicated by white arrows) marked by MAP2 antibody staining (the top panel) with amyloid-loaded axons (indicated by yellow arrows) marked by Aβ immunostaining (the bottom two panels). A senile plaque in the bottom panel was labeled with an asterisk. **C**. Imaging measurements showed that Aβ-positive axon diameters (N=200) were around 1.72±0.52 fold of control axons (N=34) and the difference is statistically significant ($p<0.001$, Mann-Whitney test). Scale bar, 50 μm.

**Axons in AD patients showed a reduction of structural protein MAP2**

To examine the effect of axon amyloidosis on the neurons, AD brain sections was also stained with the antibody against MAP2, a microtubule-associated structural protein highly expressed in the neuron soma and axons. Although a quantification of MAP2 expression in the whole brain is difficult to perform, the presented example showed that there was a significant loss of MAP2 staining in axons (MAP2-postive axon numbers decreased more than half as estimated from Figure 2A) in AD frontal brain tissues when examining from both longitudinal and transverse orientation, while the MAP2 expression in the soma of AD neurons appeared less affected. Double immunostaining with Aβ antibody showed that MAP2 expression inversely correlated with Aβ staining on the axons in AD brain tissues (Figure 2B). In the AD white matter, many axons showed a loss of MAP2 protein while bearing significant Aβ staining. MAP2 staining

227 on Aβ-positive axons was often fragmented and diffusive. Within dense-core senile
228 plaques, there is usually very little MAP2 immunostaining.

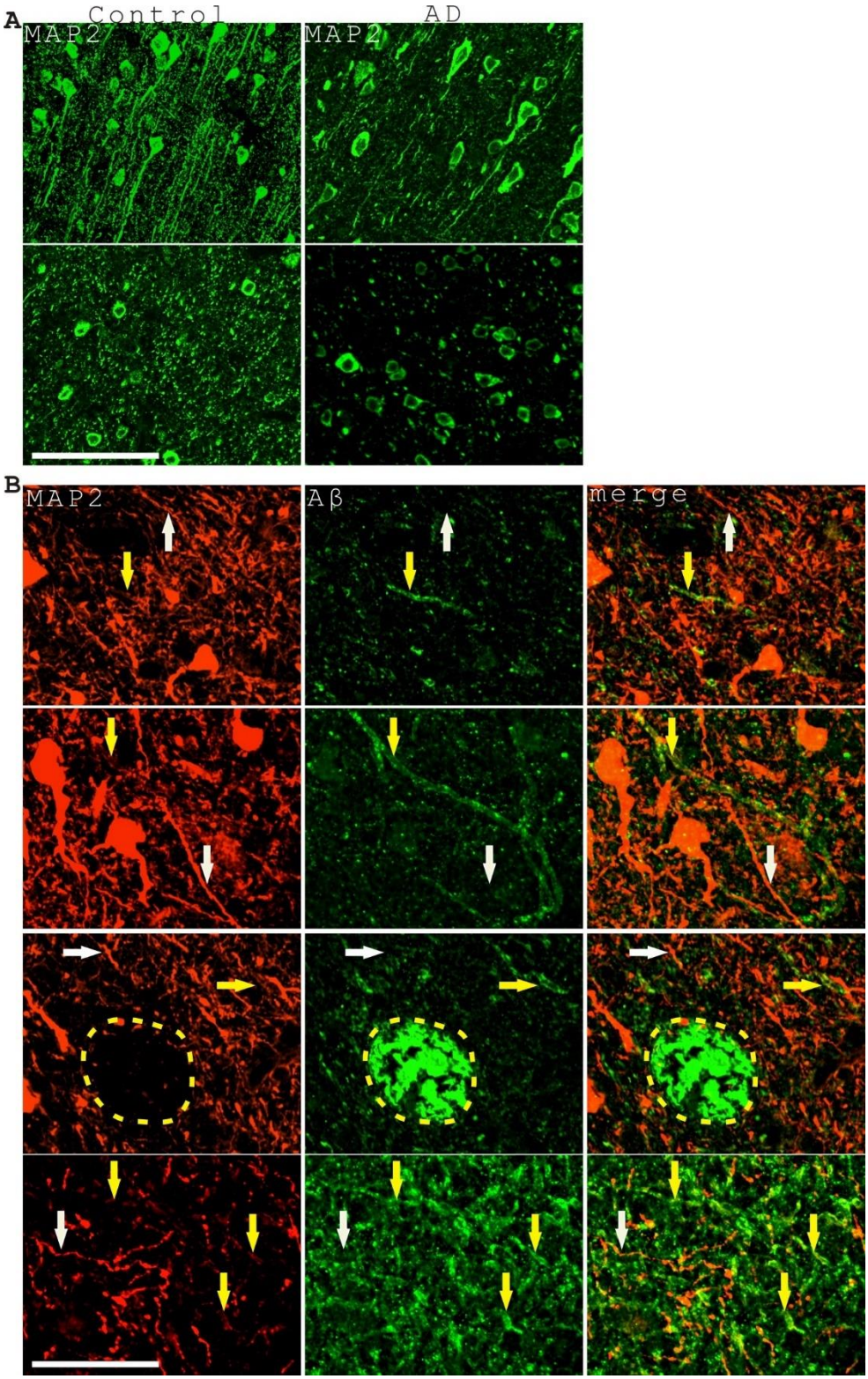


229

230 **Figure 2. Axons in the AD frontal brain tissues showed a loss of axon structural**
231 **protein MAP2. A**. At both longitudinal (top panel) and transverse orientation (bottom

panel), a significant loss of MAP2 protein was detected in the axons in the AD brain tissues comparing to control brain tissues. Scale bar, 100 μm. **B.** Four representative images showed that the loss of axonal MAP2 expression was correlated with increased Aβ immunostaining in axons in AD brain tissues. The top three images showed axons in the grey matter while the bottom image showed many Aβ-loaded axons with diminished MAP2 staining in the white matter. Aβ-positive axons were indicated with yellow arrows while Aβ-negative axons were indicated with white arrows. The yellow dashed-lines circled a dense-core senile plaque with barely detectable MAP2 immunostaining. Scale bar, 50 μm.

**Lysosomal destabilization was detected in AD frontal brain tissues**

We hypothesized that the loss of MAP2 protein in axons might be due to some faulty protein degradation events. Lysosomes and proteasome pathways are major pathways of protein degradation. Since we observed that Aβ-positive axons appear to contain many vesicles, we stained the sections with lysosomal enzyme marker Cathepsin D. Although previously we identified some weak extracellular Cathepsin D staining coming together with senile plaque Aβ aggregates, we also observed intracellular neuronal lysosome Cathepsin D staining clearly[3]. However, neuronal Cathepsin D staining was not homogeneous. Instead, we frequently observed abnormal Cathepsin D staining in the senile plaque regions (Figure 3). Normal lysosomal staining showed granule-like patterns with strong Cathepsin D signals. Conversely, nearly half of the lysosomal compartments in senile plaques showed abnormal Cathepsin D staining with enlarged, diffusive and weak staining patterns, indicating that lysosomal Cathepsin D leakage might be happening, which is a character of lysosome destabilization according to previous literatures[9-11]. A weak but detectable Aβ staining could be observed in these abnormal lysosomal compartments. We measured the sizes and intensities of lysosomal compartments within senile plaque regions comparing to lysosomes outside of senile plaque regions. The lysosomal compartments (including all Cathepsin D-labeled compartments) within the senile plaques are roughly 3.65±1.68 ($p<0.001$) times

larger by diameter (122 lysosome compartments within senile plaque regions vs 60 lysosomes outside of plaque regions) and characterized by considerably weaker Cathepsin D staining intensity (0.76±0.3 ($p<0.001$)). In AD axons, Aβ and lysosomal enzyme marker Cathepsin D are highly co-localized, showing the predominant presence of axonal Aβ in the lysosomes. (indicated by white arrows in Figure 3D-F). We also detected diffusive and weaker Cathepsin D staining patterns along the length of Aβ-positive axons, suggesting axonal lysosome destabilization (indicated by yellow arrows). We think that the destabilized lysosomes with lysosome enzyme leakage might contribute to the loss of MAP2 protein in the axons.

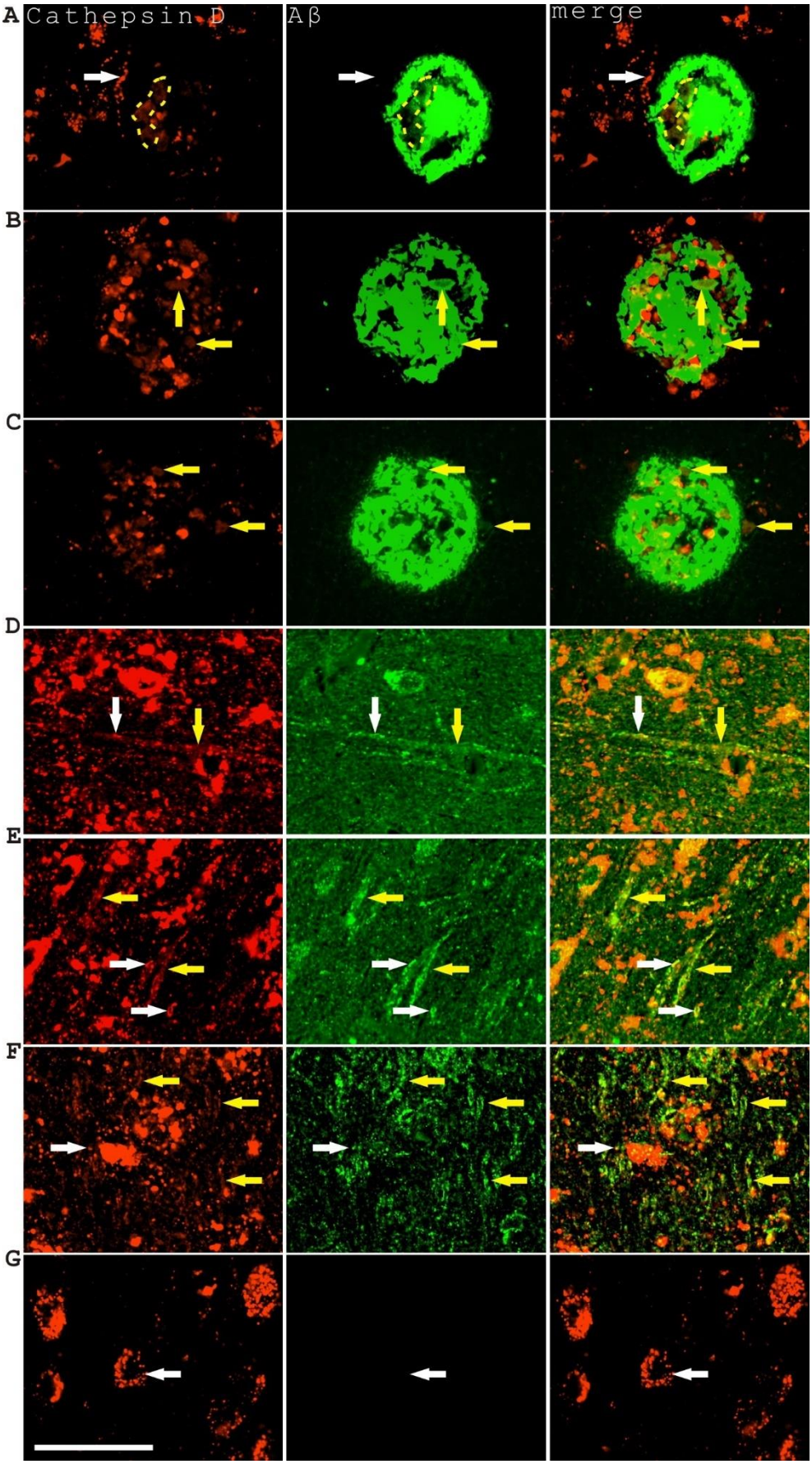


272

273

**Figure 3. Lysosomal destabilization was common in AD frontal brain tissues.** Three plaques were shown (**A-C**). The top plaque was a typical dense-core plaque while the bottom two plaques were more diffusive. All three plaques associated with enlarged and diffusive Cathepsin D staining patterns (yellow dashed lines or yellow arrows), a character of lysosome destabilization and lysosome permeabilization comparing to typical, granule-like strong lysosome staining with focal Cathepsin D positivity (indicated with white arrows in the top panel). Weak Aβ staining could be observed in these abnormal lysosomal compartments. (**D-F**) showed three representative images illustrating the diffusive Cathepsin D staining in the Aβ-positive axons (indicated with yellow arrows). At the same time, the co-localization between Aβ and Cathepsin D in lysosomes was abundantly observed (indicated with white arrows). It should be noted that these three pictures were taken with longer exposure settings in order to show the weak axonal Aβ and Cathepsin D staining comparing to other pictures. **G**. intracellular lysosomes away from amyloid plaques showed typical, strong and granule-like lysosomal Cathepsin D staining (indicated with white arrows). Scale bar, 50 μm.

**Destabilized lysosomes were located in dystrophic neurites**

To further prove that these destabilized lysosomal staining was linked to axon degeneration, we stained the tissue sections with phosphorylated Tau (phos-Tau) antibody, a well-known axon dystrophy marker in the Alzheimer's disease, and the lysosomal membrane marker Lamp2. The co-localization between abnormally diffusive lysosomal Lamp2 staining with dystrophic neurites, neurofibrillary tangles, neuropil threads was observed (Figure 4A). When we stained the AD brain sections with both phos-Tau and Aβ, the co-localization between phos-Tau and Aβ was also detected in dystrophic neurites in senile plaques, neurofibrillary tangles and axons (Figure 4B). However, Aβ staining in dystrophic neurites, tangles and axons was very low comparing to the strong Aβ staining in the senile plaques. These data confirmed that axon dystrophy connected with Aβ, Tau phosphorylation and lysosome destabilization.

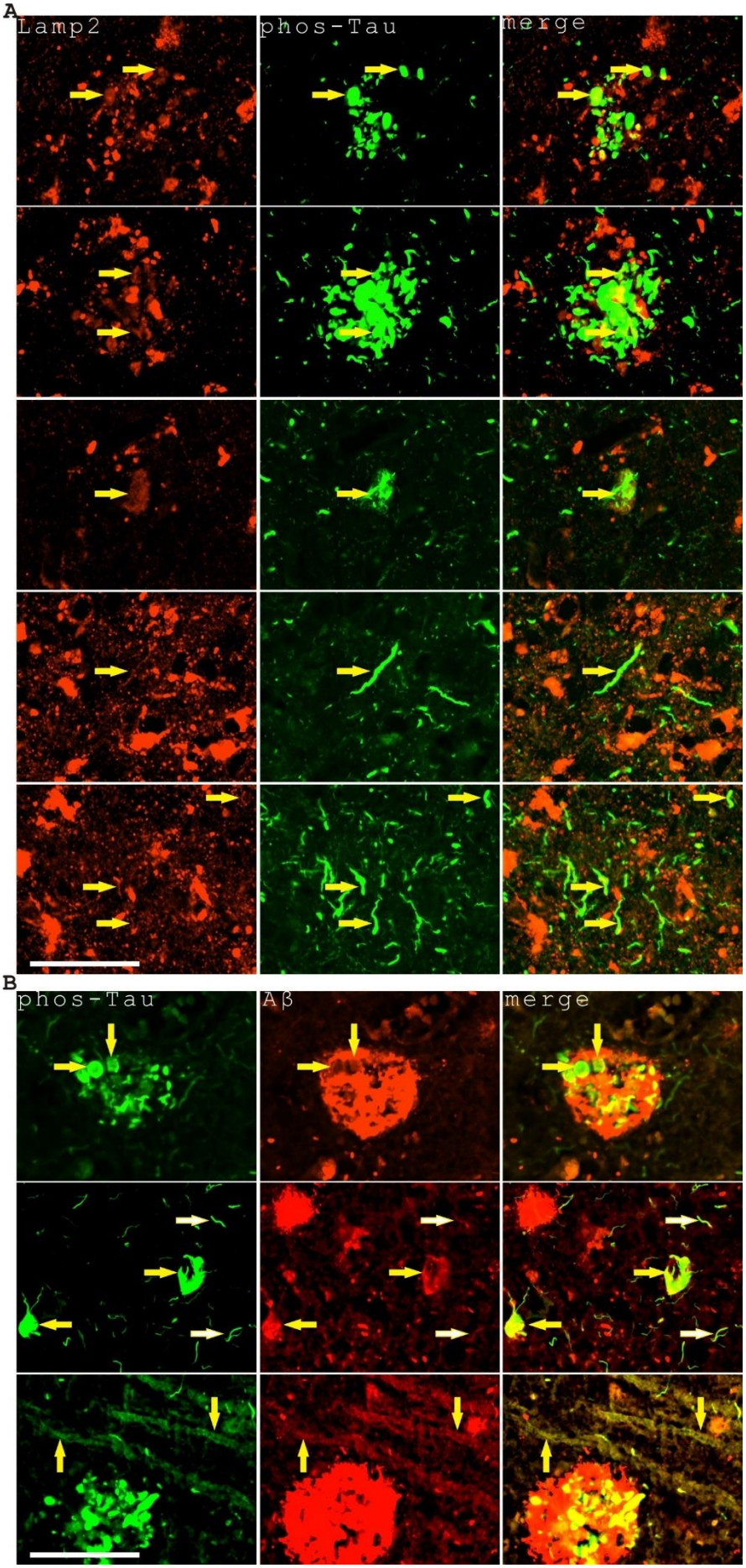
A
Lamp2
phos-Tau
merge
B
phos-Tau
Aβ
merge

**Figure 4. Destabilized lysosomes were located in dystrophic neurites, neurofibrillary tangles and neuropil threads, additionally there is a co-distribution between Tau phosphorylation and intracellular Aβ staining in dystrophic neurites, tangles and axons. A**. Abnormal lysosome Lamp2 staining (indicated with arrows) was detected in dystrophic neurites (top two panels), tangles (the third panel) and neuropil threads (the bottom two panels) marked with phos-Tau immunostaining. Particularly, we observed long, diffusive but relatively weaker Lamp2 staining along the length of multiple neuropil threads, highlighting the intricacy of this defect. Scale bar, 50 μm. **B**. phos-Tau-positive dystrophic neurites (top panel), tangles and neuropil threads (middle panel) and axons (bottom panel) were also Aβ-positive (indicated with arrows). Scale bar, 50 μm.

**Axon degeneration in AD bears the markers of hemorrhagic insults**

It is not very clear why axons in AD tissues are degenerating. It has been shown that Aβ oligomers can cause beading-type degeneration analogous to spheroid formation and also lysosome destabilization in cell culture experiments[10, 12]. However, in the *in vivo* situations, Aβ alone might not be fully responsible for the degenerating effect since Aβ is interacting with many other proteins. As our previous research suggested that senile plaques are formed by blood Aβ leakage into the brains upon microaneurysm leakage, we hypothesized that axon damages in AD tissues might be also associated with many blood-related proteins. We checked the axon pathology with a variety of blood or plasma-related markers. The results showed that axons in AD brains indeed carried blood and plasma markers such as ApoE, HBA, HbA1C and Hemin (Figure 5A-D). It appears that the presence of blood markers in the axons is not depending on the spatial closeness to the senile plaques. In addition, the distribution of hemorrhagic markers is not always quantitively proportional to the intensity of Aβ in the AD brain tissues. Sometimes there is even stronger staining of hemorrhagic markers in the axons than in the surrounding senile plaques, which is likely because of the differential enrichment of amyloid protein complexes in axons vs. senile plaques (an example was

334 shown in the top panel of Figure 5D with more Hemin staining in the axons than in the
335 adjacent senile plaque). Moreover, axon amyloidosis is associated with the expression
336 of Sortilin1, another endosomal/lysosomal marker (Figure 5E), which has also been
337 implicated as a major receptor for ApoE[13]. Furthermore, when we stained the sections
338 with red blood cell related histological stains such as Alizarin red and Rhodanine, we
339 could also see many axons in the AD brain tissues positively stained by these stains
340 (Supplementary Figure 1). All these analyses indicated that the axons not only were
341 enriched for Aβ but also enriched for many hemorrhage-related markers. Since
342 intracellular Aβ mostly existed in the lysosomes as shown in Figure 3, the above data
343 also suggested that intracellular ApoE, HBA, HbA1C and Hemin primarily located in
344 the lysosomes.

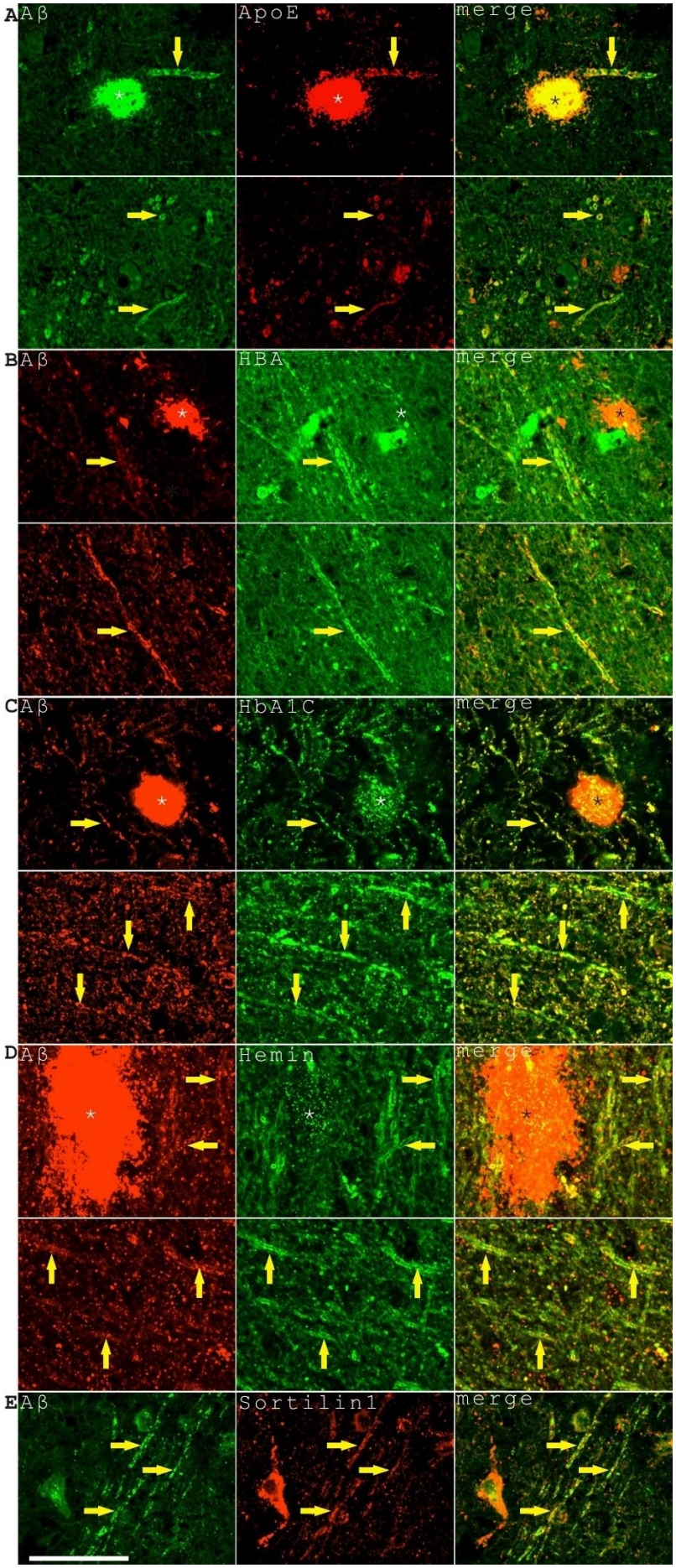
A
Aβ
ApoE
merge
B
Aβ
HBA
merge
C
Aβ
HbA1C
merge
D
Aβ
Hemin
merge
E
Aβ
Sortilin1
merge

**Figure 5. Axon degeneration in AD bears the markers of hemorrhagic insults.** Four blood-related markers (ApoE, HBA, HbA1C, Hemin) all showed positivity in enlarged axons labeled with Aβ immunostaining, that can be adjacent to senile plaques or not associated with senile plaques (**A** to **D**). Degenerating axons were also positive for an endosomal/lysosomal marker Sortilin1 (**E**). The affected axons were indicated by arrows while the senile plaques were indicated with asterisks. Scale bar, 50 μm.

**Under rare occasions, axon breakages were observed in AD brain tissues**

Whether the axonal degeneration defects will ultimately lead to axon breakages in the Alzheimer's disease is an important question to be addressed. We checked hundreds of images containing Aβ-stained axons. We initially focused on axons traveling in the longitudinal orientation inside of senile plaques since the axons in the transverse orientation were difficult to be identified. We observed that many axons passing through the senile plaques were Aβ-positive and enlarged but they did not break (Supplementary Figure 2). However, we did find a few examples indicating that the axons could truly be broken at locations outside of senile plaques. Using Aβ and AGE antibody as the markers for amyloidosis-affected axons, broken axons with gaps up to 38.4 μm in width could be detected (Figure 6A). What caused these rare axon breakages is not immediately clear. On the other hand, we observed that long stretches of amyloid-loaded vesicles with large spheroid formation on the axons caused dramatic dystrophy to a degree that the axon morphology could no longer be recognized (Figure 6B). The long stretch clustering of vesicles with spheroid formation was likely due to lysosome clustering as indicated by the endosome/lysosomal marker Sortilin1 (Figure 6C). It is possible that the continuous enlargement of destabilized lysosomal compartment across long distance might finally result in axon breakages in some cases.

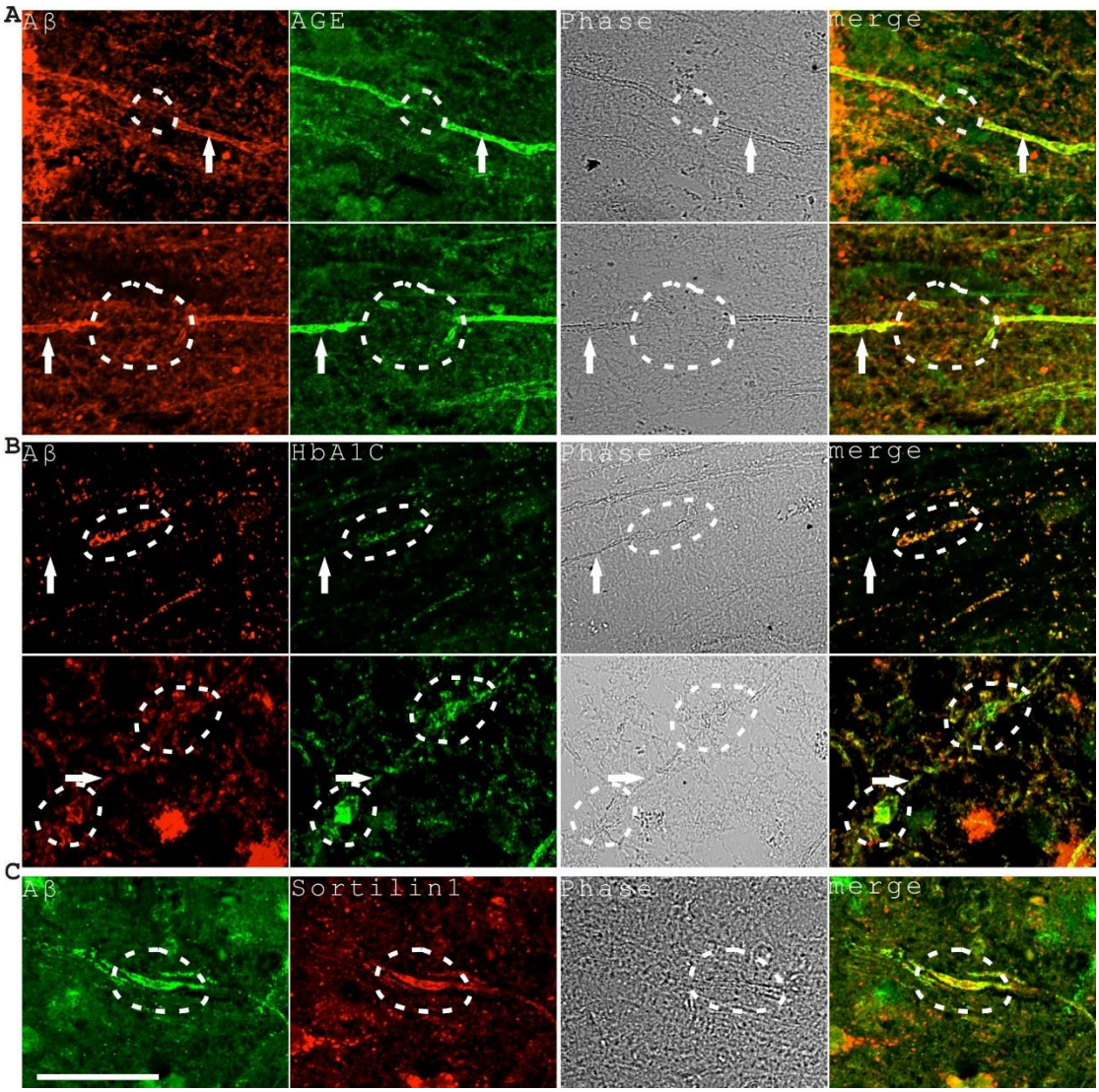


**Figure 6. Under rare occasions, axon breakages were observed in AD brain tissues.** **A**. Two broken axons were identified with AGE and Aβ immunohistochemistry in AD brain tissues. The axonal gap in the top image was measured around 24.4 μm while in the bottom image was measured around 38.4 μm. The broken regions were marked with dashed lines while the parental axons were indicated with arrows. **B**. Two examples of damaged axons associated with large vesicle clusters and spheroid formation enriched for amyloid markers Aβ and HbA1C. The long stretch of clustered vesicles (indicated with dashed lines) in the top panel measured around 32.5 μm in length. The maximal width of the two large spheroids (indicated with dashed lines) in the bottom panel reached 6.2 μm (top-right position) and 8.3 μm (bottom-left position) respectively. The affected axons were indicated with arrows. **C**. A long axonal region (indicated with dashed lines) with large spheroid formation associated with endosomal/lysosomal

387 domains marked with Sortilin1 immunostaining. This region was measured around 26.1
388 μm in length. The maximal width of the spheroid measured around 4.1 μm. Scale bar,
389 50 μm.
390
391 **Discussion:**
392
393 The reason that axonal Aβ staining was not clearly observed in our previous studies[3,
394 8] is likely because the strong senile plaque Aβ staining camouflages the fainter staining
395 of axonal Aβ. The widespread axonal enlargement associated with Aβ deposition might
396 have a significant influence on the AD pathology and its dementia phenotypes. It has
397 been shown that in the natural animal species, axons with larger diameter have higher
398 transduction speed, for example, in the case of the squid giant axon[14]. However, in
399 the case of AD, the enlarged axons were not natural but instead pathological, which
400 were filled with toxic Aβ, hemolytic proteins and destabilized lysosomes. In addition,
401 lysosomal leakage can cause axonal structural damages and increase axolemmal
402 permeability, which might further damage the myelin sheath. Both human and mouse
403 studies indicated that axon diameter increases with aging and cognition decline[15, 16].
404 There is also a reduced velocity of action potential transmission in AD patients and AD-
405 model transgenic mice[17, 18]. Diffusion tensor imaging studies also indicated that
406 structural damage and disconnection in the white matter is prominent in AD patients[19,
407 20]. Axonal amyloidosis and enlargement in AD are likely linked to transduction
408 velocity decrease and white matter damage phenotypes. Besides the basic axonal
409 enlargement phenotype in AD, spheroid formation is also frequently observed. Previous
410 studies showed that spheroid formation on axons also slows down the speed of action
411 potential transduction[21, 22]. All these studies showed strong evidence that there are
412 serious axonal defects in AD with transduction speed decline as a central phenotype.
413 How and to what extent Aβ deposition in enlarged axons impacts on the whole brain
414 connectome function requires further large-scale quantitative analysis and *in vivo*
415 animal and human studies.
416

Axonal amyloidosis additionally induces axonal structural changes such as a loss of MAP2 protein, which might be due to Aβ toxicity in inducing lysosomal destabilization. It has been shown *in vitro* that extracellular Aβ was taken up and concentrated in lysosomes and induced lysosome destabilization and permeabilization[10, 11]. Lysosome permeabilization has been studied in mouse AD models and was considered as the possible mechanism for neuronal cell death and senile plaque formation[23]. In our opinion, Aβ could be classified as a type of lysosomal "toxin", which exerts its unique toxicity after lysosomal intake and processing. However, the current study indicated that lysosomal destabilization might not be due to Aβ alone since axonal amyloidosis associated with the enrichment of multiple hemorrhagic markers such as ApoE, HBA, HbA1C and Hemin, which are also major binding partners of Aβ[3, 8, 24, 25]. Axonal amyloidosis also associated with Sortilin1 expression. Sortilin1 is an endosome/lysosome marker that has been identified as a major receptor of ApoE[13]. Although Aβ accumulation in axons may be related to disrupted axonal transport[26], axons might additionally take up exogeneous Aβ complexes through receptor-related mechanisms, independent of the neural soma, by the relay chains starting from Aβ to ApoE then to Sortilin1. The intake of a large number of hemolytic proteins along with Aβ could possibly induce severe axonal proteostatic stress besides the toxicity effects of Aβ.

Both Aβ deposition and Tau phosphorylation are important components of AD pathology, however, how these two events connect is not clear. Previously, it has been suggested that Aβ and Tau co-localize in AD "synaptosomes"[27]. In this study, we provide another possible answer that Aβ and Tau are both connected to destabilized lysosomes. There is ample evidence that Aβ endocytosis induces lysosome destabilization[9, 10, 28]. There is also strong evidence that Aβ likely induces Tau phosphorylation[29, 30]. We show in this study that Tau phosphorylation also associates with destabilized lysosomes in tangles, dystrophic neurites and also neuropil threads. It is not known whether Tau phosphorylation or lysosome destabilization is the upstream event. However, if taking into account for the MAP2 loss in axons and the evidence in

the literature that MAP2 competes with Tau for microtubule binding[31] and could prevent Tau aggregation[32], lysosomal destabilization might work upstream of Tau phosphorylation by chronically degrading its competitive inhibitor MAP2.

Under rare occasions, the breakage of axons has been observed in a small number of axons in our experiments. When axon breakages happen and are not repaired, Wallerian degeneration of axons might occur, which could result in axon loss. Since small axon breakages are difficult to detect, the actual axonal breakage events in AD brains might be more abundant than what we observed. How frequently the axonal breakages and Wallerian degeneration happen in the AD brains requires further investigation. Both Wallerian degeneration and axon regeneration are affected by various gene mutations[33-35]. To combat Alzheimer's disease efficiently, firstly, we need to find ways to prevent microvascular blood leakage and axonal accumulation of Aβ and hemorrhagic proteins. Secondly, treatments that can specifically slow down Wallerian degeneration and facilitate axon repair, reconnection and regeneration are also likely strongly beneficial for AD patients.

**References:**


1. Hardy, J.A. and G.A. Higgins, *Alzheimer's disease: the amyloid cascade hypothesis.* Science, 1992. **256**(5054): p. 184-5.
2. Lane, C.A., J. Hardy, and J.M. Schott, *Alzheimer's disease.* European Journal of Neurology, 2018. **25**(1): p. 59-70.
3. Fu, H., et al., *Senile plaques in Alzheimer's disease arise from Aβ- and Cathepsin D-enriched mixtures leaking out during intravascular haemolysis and microaneurysm rupture.* FEBS Lett, 2023. **597**(7): p. 1007-1040.
4. Cras, P., et al., *Senile Plaque Neurites in Alzheimer-Disease Accumulate Amyloid Precursor Protein.* Proc Natl Acad Sci U S A, 1991. **88**(17): p. 7552-7556.
5. Tsai, J., et al., *Fibrillar amyloid deposition leads to local synaptic abnormalities and breakage of neuronal branches.* Nature Neuroscience, 2004. **7**(11): p. 1181-1183.
6. Braak, H. and K. Del Tredici, *Amyloid-β may be released from non-junctional varicosities of axons generated from abnormal tau-containing brainstem nuclei in sporadic Alzheimer's disease: a hypothesis.* Acta Neuropathologica, 2013. **126**(2): p. 303-306.
7. Fu, H., et al., *Persisting and Increasing Neutrophil Infiltration Associates with Gastric Carcinogenesis and E-cadherin Downregulation.* Sci Rep, 2016. **6**: p. 29762.
8. Fu, H.L., et al., *Aβ-Aggregation-Generated Blue Autofluorescence Illuminates Senile*

*Plaques as well as Complex Blood and Vascular Pathologies in Alzheimer's Disease.* Neuroscience Bulletin, 2024.

9. Takahashi, R.H., et al., *Intraneuronal Alzheimer abeta42 accumulates in multivesicular bodies and is associated with synaptic pathology.* The American journal of pathology, 2002. **161 5**: p. 1869-79.
10. Liu, R.Q., et al., *Membrane localization of beta-amyloid 1-42 in lysosomes: a possible mechanism for lysosome labilization.* J Biol Chem, 2010. **285**(26): p. 19986-96.
11. Zaretsky, D.V., M.V. Zaretskaia, and Y.I. Molkov, *Membrane channel hypothesis of lysosomal permeabilization by beta-amyloid.* Neurosci Lett, 2022. **770**: p. 136338.
12. Alobuia, W.M., W. Xia, and B.P. Vohra, *Axon degeneration is key component of neuronal death in amyloid-β toxicity.* Neurochem Int, 2013. **63**(8): p. 782-9.
13. Carlo, A.S., et al., *The pro-neurotrophin receptor sortilin is a major neuronal apolipoprotein E receptor for catabolism of amyloid-β peptide in the brain.* J Neurosci, 2013. **33**(1): p. 358-70.
14. Hartline, D.K. and D.R. Colman, *Rapid conduction and the evolution of giant axons and myelinated fibers.* Curr Biol, 2007. **17**(1): p. R29-35.
15. Fan, Q., et al., *Age-related alterations in axonal microstructure in the corpus callosum measured by high-gradient diffusion MRI.* NeuroImage, 2019. **191**: p. 325-336.
16. Parandavar, E., et al., *Long-term demyelination and aging-associated changes in mice corpus callosum; evidence for the role of accelerated aging in remyelination failure in a mouse model of multiple sclerosis.* Aging Cell, 2024. **n/a**(n/a): p. e14211.
17. Qian, X., et al., *Reduced Peripheral Nerve Conduction Velocity is Associated with Alzheimer's Disease: A Cross-Sectional Study from China.* Neuropsychiatr Dis Treat, 2022. **18**: p. 231-242.
18. Gelman, S., J. Palma, and A. Ghavami, *Axonal Conduction Velocity in CA1 Area of Hippocampus is Reduced in Mouse Models of Alzheimer's Disease.* J Alzheimers Dis, 2020. **77**(4): p. 1383-1388.
19. Chen, Y., et al., *Abnormal white matter changes in Alzheimer's disease based on diffusion tensor imaging: A systematic review.* Ageing Research Reviews, 2023. **87**: p. 101911.
20. Fellgiebel, A. and I. Yakushev, *Diffusion tensor imaging of the hippocampus in MCI and early Alzheimer's disease.* J Alzheimers Dis, 2011. **26 Suppl 3**: p. 257-62.
21. Kolaric, K.V., et al., *Focal axonal swellings and associated ultrastructural changes attenuate conduction velocity in central nervous system axons: a computer modeling study.* Physiol Rep, 2013. **1**(3): p. e00059.
22. Yuan, P., et al., *PLD3 affects axonal spheroids and network defects in Alzheimer's disease.* Nature, 2022. **612**(7939): p. 328-337.
23. Lee, J.-H., et al., *Faulty autolysosome acidification in Alzheimer's disease mouse models induces autophagic build-up of Aβ in neurons, yielding senile plaques.* Nature Neuroscience, 2022. **25**(6): p. 688-701.
24. Golabek, A., et al., *Amyloid β binding proteins in vitro and in normal human cerebrospinal fluid.* Neuroscience Letters, 1995. **191**(1): p. 79-82.
25. Chuang, J.Y., et al., *Interactions between amyloid-β and hemoglobin: implications for amyloid plaque formation in Alzheimer's disease.* PLoS One, 2012. **7**(3): p. e33120.
26. Nukina, N., et al., *Accumulation of amyloid precursor protein and beta-protein*

*immunoreactivities in axons injured by cerebral infarct.* Gerontology, 1992. **38 Suppl 1**: p. 10-4.

27. Fein, J.A., et al., *Co-localization of amyloid beta and tau pathology in Alzheimer's disease synaptosomes.* Am J Pathol, 2008. **172**(6): p. 1683-92.
28. Tam, J.H.K., C. Seah, and S.H. Pasternak, *The Amyloid Precursor Protein is rapidly transported from the Golgi apparatus to the lysosome and where it is processed into beta-amyloid.* Molecular Brain, 2014. **7**(1): p. 54.
29. Zheng, W.H., et al., *Amyloid beta peptide induces tau phosphorylation and loss of cholinergic neurons in rat primary septal cultures.* Neuroscience, 2002. **115**(1): p. 201-11.
30. Mattsson-Carlgren, N., et al., *Aβ deposition is associated with increases in soluble and phosphorylated tau that precede a positive Tau PET in Alzheimer's disease.* Sci Adv, 2020. **6**(16): p. eaaz2387.
31. Sandoval, I.V. and J.S. Vandekerckhove, *A comparative study of the in vitro polymerization of tubulin in the presence of the microtubule-associated proteins MAP2 and tau.* J Biol Chem, 1981. **256**(16): p. 8795-800.
32. Holden, M.R., et al., *MAP2 caps tau fibrils and inhibits aggregation.* J Biol Chem, 2023. **299**(7): p. 104891.
33. Coleman, M.P. and M.R. Freeman, *Wallerian degeneration, wld(s), and nmnat.* Annu Rev Neurosci, 2010. **33**: p. 245-67.
34. Teoh, J.S., et al., *Bridging the gap: axonal fusion drives rapid functional recovery of the nervous system.* Neural Regen Res, 2018. **13**(4): p. 591-594.
35. Neumann, B., et al., *Axonal regeneration proceeds through specific axonal fusion in transected C. elegans neurons.* Dev Dyn, 2011. **240**(6): p. 1365-72.

Supplementary Information for

# Pathological axonal enlargement in connection with amyloidosis, lysosome destabilization and hemorrhage is a major defect in the Alzheimer's disease

Hualin Fu, Jilong Li, Chunlei Zhang, Guo Gao, Qiqi Ge, Xinping Guan, Daxiang Cui

**This PDF file includes:**

Supplementary Fig. 1 and 2

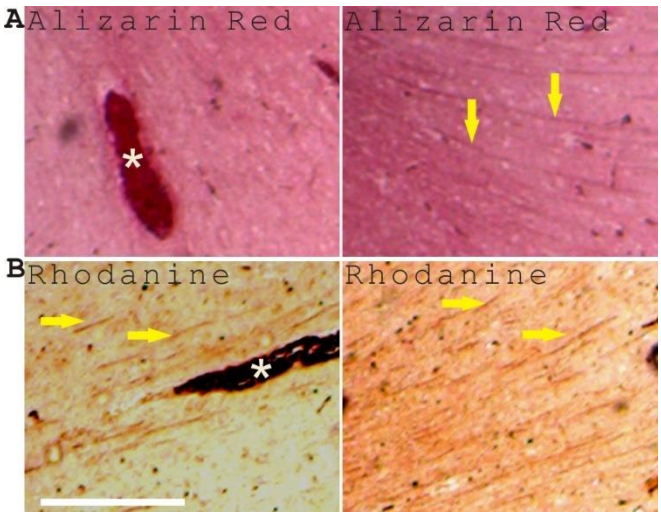


**Supplementary Figure 1. Many axons were positively stained by Alizarin Red and Rhodanine in the AD brain tissues. A.** This panel showed that Alizarin red positively stained the red blood cells and also axons. **B**. This panel showed that Rhodanine also stained the red blood cells and axons positively. Red blood cells in the blood vessels were marked with asterisks while the axons were indicated with arrows. Scale bar, 100 μm.

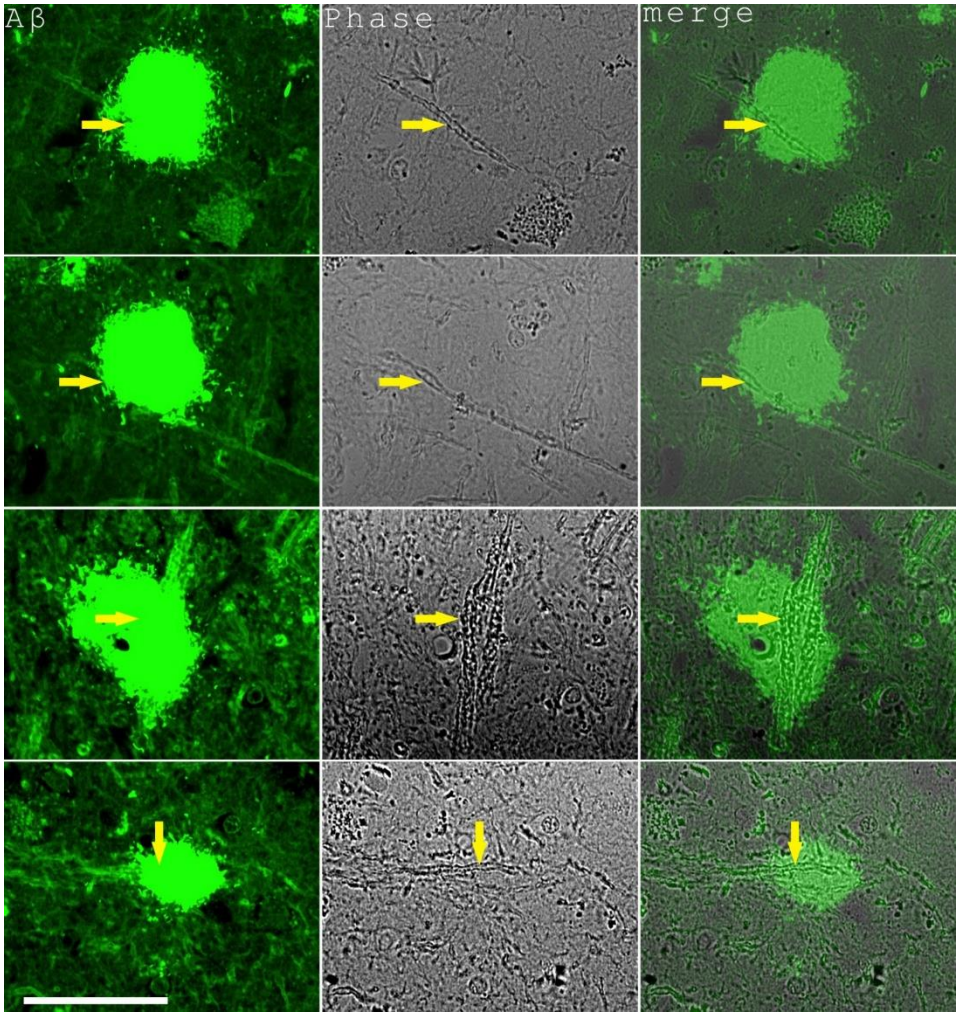


**Supplementary Figure 2. Enlarged axons（indicated with arrows）were detected inside of senile plaques but axon breakage was not observed.** Four representative images were shown. Scale bar, 50 μm.